Macromolecular Materials and Engineering
www.mme-journal.de

Synthesis and Characterization of CNT Composites for Laser-Generated Ultrasonic Waves

Patrick Oser, Oliver Düttmann, Fabian Schmid, Levin Schulte-Spechtel, Christian U. Große,* and Datong Wu**

In the last few years, extensive progress in ultrasonic wave generation by using multiwalled carbon nanotubes (MWCNTs) in combination with polydimethylsiloxane (PDMS), functional composites, has been achieved. Due to high optical absorption of MWCNTs as perfect absorbers for laser beams and the high thermal expansion coefficient of PDMS, a compact transducer for ultrasonic wave generation at higher frequency can be realized. This study reports a novel method to synthesize MWCNT–PDMS composites deposited on a glass substrate by spray coating, which is done in a short time of 2 h. The layers (0.9–32.2 µm) show low optical transmission properties of 13.9–0.0% at a wavelength of 1047 nm. Apart from using a 1% Triton-X-100 stock solution and then diluted to a 0.1% relatively nonhazardous solution, no toxic chemicals are used. The Triton-X-100 solution is not hazardous for lab handling and is a commonly used lab detergent for the treatment of biological cells. The achieved sound pressure level is 3.4 MPa with a frequency bandwidth of 9.7 MHz. These results show the potential for a fast and nontoxic production of laser-generated ultrasonic transducers, which can be used well in the field of nondestructive material testing of layered materials or in medicine with an appropriate frequency range.

1. Introduction

Since many years, photoacoustic applications have offered far-reaching imaging possibilities in nondestructive material testing and in medicine. Photoacoustics describes the conversion of absorbed laser energy into sound waves in a medium. Based on the photoacoustic effect ultrasonic waves can be generated by the laser induced thermal expansion of the samples. The method has some limitations in applications on sensitive materials like living tissues since the risk for burns or ablation from excessive heat limits the amount of used energy. Piezoelectric ultrasonic actuators are often used today for generation of ultrasonic waves, although their effective bandwidth is limited, and they are susceptible to electromagnetic interferences.

In addition, at high ultrasonic frequency miniaturization of piezoelectric transducers requires a great deal of effort in their precise production of very small structures, narrow spacing and complex dice and fill technique for piezoelectric composites arrays.[1–4] On the other hand, the transducer sensitivity depends on active transducer area, which drops when reducing the area size of piezoelements. A new kind of laser based ultrasonic generators has been developed and investigated during the last years as an extension and alternative to classical photoacoustic and piezoelectric applications.[5–10] A sample is not directly illuminated by a laser pulse, but a robust intermediate layer, which absorbs laser energy and converts to sound pressure waves. The thin layers have a high optical absorption,[11] a high thermal expansion coefficient and can withstand high laser powers, which therefore emits higher sound pressure waves without damaging the sample. The design varies from pure nanoparticle coatings or metal layers [5,12–17] to the combination of different nanoparticles with polymers.[2,11,18,19] The nanoparticles work as intermediate agents between the heat generated in the nanoparticles by optical absorption and, e.g., the polymer with a high thermal expansion. Various research groups have investigated various nanoparticles for this application in detail for several years. For the purpose of high optical absorption, gold nanostructures,[20–22] graphite,[5,19] carbon fibers,[8,23] carbon black [18,24] as well as candle soot [25–27] have been investigated so far. Other highly absorbing nanoparticles are carbon nanotubes (CNTs), which are promising for these applications,[2,10,28] as they show the highest optical absorption properties in a broad range of optical wavelengths.[29–32] The efficiency for ultrasonic generation can be improved by an elastomer component such as polydimethysiloxane (PDMS), since PDMS shows a large volumetric thermal expansion coefficient ($\beta = 300 \times 10^{-6}$ C^{-1})[33–35] and at the same time low optical absorption.[36,37] The integration of nanoparticles in a polymer can be challenging, but necessary, as they

P. Oser, O. Düttmann, F. Schmid, L. Schulte-Spechtel, Prof. D. Wu
Department of Applied Sciences and Mechatronics
University of Applied Sciences Munich
Lothstraße 34, Munich 80335, Germany
E-mail: patrick.oser@hm.edu; datong.wu@hm.edu

Prof. C. U. Große
Department of Civil
Geo and Environmental Engineering
Chair of Non-Destructive Testing
Technical University of Munich
Baumbachstr. 7, Munich 81245, Germany
E-mail: grosse@tum.de

The ORCID identification number(s) for the author(s) of this article can be found under https://doi.org/10.1002/mame.201900852.

DOI: 10.1002/mame.201900852

can significantly improve physical properties of layers, such as average thermal conductivity.[38] Major efforts have been aimed at achieving a homogeneous distribution of nanoparticles in, e.g., polymers.[9,39–43] Because of van der Waals forces,[44–46] carbon nanotubes tend to reconglomerate. Efforts to prevent reconglomeration range from various chemical functionalization and derivatization [9,39] to strong mechanical processing methods, such as ultrasonic treatments and mechanical stirring.[43] The mechanical processing methods can damage the nanotubes [43,47,48] and cause them to lose their physical properties. Processing methods of carbon nanotube-based functional layers are complex and include the use of partly toxic and harmful chemicals and can also cause damage to the nanotubes.[49]

In this study, we present an improved alternative method for the synthesis of high concentrated MWCNT–PDMS composites, with high optical absorption property. These methods include determining the photoacoustic performance, robustness of the layers, and the investigation of the homogeneous distribution of MWCNTs in PDMS. The fabrication process was carried out by applying thin MWCNT–PDMS layers on a glass substrate by spray coating with an airbrush gun. Apart from using a 1% Triton-X-100 stock solution and then diluted to a 0.1% relatively nonhazardous solution, no toxic chemicals were used. The developed manufacturing method for coating layers is robust, straightforward and fast (about 2 h). The thickness of the layers can be controlled by modifying the spraying time. The method presented in this work enables a precise creation of thin and high absorbing ultrasonic actuators in a short time. Due to an appropriate frequency bandwidth and pressure level, these composites can be well used in the field of nondestructive material testing of layered materials or in medicine.

2. Experimental Section

2.1. Materials

MWCNT provided by Sigma Aldrich (724769-100G) were produced by chemical vapor deposition (CVD) using cobalt and molybdenum as catalysts (CoMoCAT). The outer diameters of the MWCNTs are 6–9 nm, the length 5 µm and they consist of at least 95% carbon.

Polyoxyethylene octyl phenyl ether (Triton-X-100) is a *p-tert*-octylphenol derivative with a polyethylene glycol side chain of 9 to 10 ethylene oxide units. It is a nonionic surfactant from the group of octylphenol ethoxylates. Sylgard 184 provided by DOW CORNING (consists of polydimethylsiloxane (PDMS) and curing agent). All chemicals are used as delivered, and no further changes were made.

2.2. Processing Methods

2.2.1. Dispersion of PDMS in Distilled Water with Triton-X-100

To evaluate the water solubility of PDMS, 4 g of PDMS was mixed in 50 mL of a 0.1% Triton-X-100 solution and homogenized in an ultrasound treatment for 30 min at 100 W at 20 kHz. It is notable, that only the PDMS part of Sylgard 184 was used without curing agent. The stable suspension after several months is shown in **Figure 1**b.

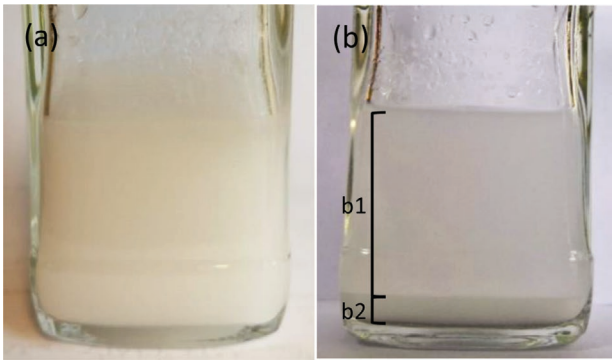

Figure 1. PDMS-Triton-X-100–water solution directly after homogenizing a) and after several months b). In (b), excessive PDMS is deposited b2) and a stable PDMS–water solution (1 mg mL^{-1}) remains b1).

After the treatment the solution was left at room temperature, until no further sedimentation takes place. In this case, the solution was kept for several months in the laboratory at room temperature. The solubility of PDMS in an aqueous 0.1% Triton-X-100 solution was determined by a gravimetric analysis. The dissolved content of PDMS in the solution (Figure 1b,b1) was measured by pipetting 5 mL in an evaporation dish and a followed treatment in a drying cabinet at 100 °C, where the water evaporated. This process was repeated after a week to validate that no further PDMS was deposited as sediment caused by movement of the solution; the following control measurements showed the same results. 1 mg mL^{-1} of PDMS can be dissolved in a 0.1% Triton-X-100 pure deionized water solution.

2.2.2. Results of CNT and PDMS Solution

Triton-X-100 is well suited for dissolving CNTs.[56–60] Therefore, it is an excellent intermediate agent between CNT and PDMS, which provides a chemically relatively nontoxic, water-soluble solution. For the preparation of a CNT–PDMS solution, a 100 mL glass bottle was filled with 45 mL of pure distilled water, 100 mg of MWCNT, and 200 mg of PDMS. To the mixture, 5 mL of a prepared 1% Triton-X-100 distilled water-based stock solution was added. The undissolved components were homogenized for 30 min with an ultrasonic homogenizer at 130 W. The highly homogenized MWCNT–PDMS solution was then very stable for the application. No sedimentation effects of MWCNTs or PDMS can be noticed after a quite long time (months).

For a homogeneous solution, a strong ultrasound treatment is necessary. A lower power treatment (below 130 W) is not sufficient to dissolve the conglomerations, which results in large lumps of undissolved CNTs (**Figure 2**).

The prepared CNT–PDMS solution was applied on a glass substrate as an ultrasonic generator for ultrasonic measurements. The deposition of the CNT–PDMS solution was done with an airbrush gun by spray coating. A 20 × 20 mm wide and 130 µm thick glass slab was used as a substrate and was placed on a hot plate (100 °C) to accelerate the evaporation process. The spraying distance was ≈30 cm from the substrate. Depending on the thickness of the

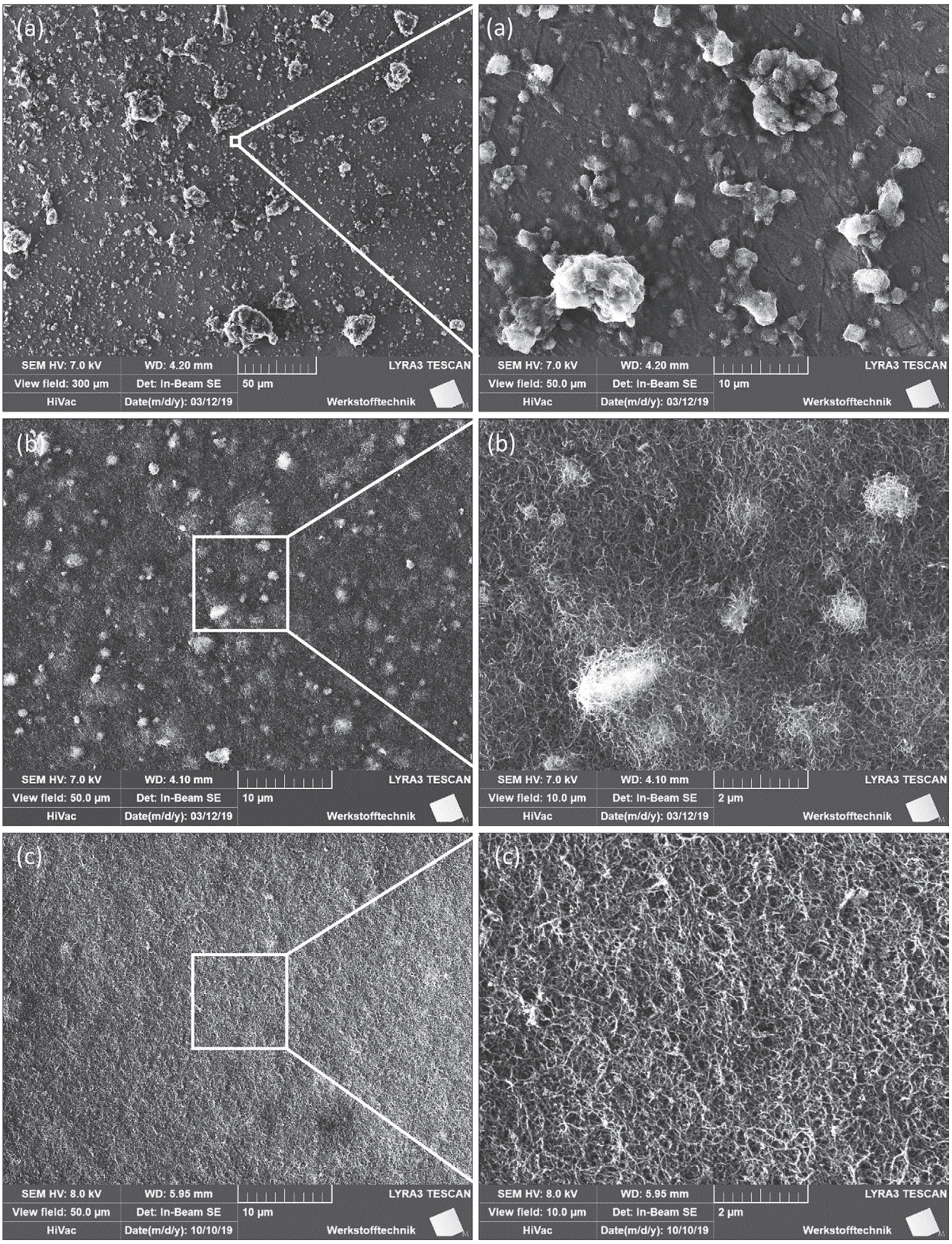

Figure 2. The effects of ultrasonic treatment for 30 min with a) 0.3 W, b) 80 W, and c) 130 W investigated with a scanning electron microscope (SEM). Panel (a) shows an image section of 50 µm and 10 µm while (b) and (c) show an image section of 10 and 2 µm. The high shear forces induced by ultrasonic waves c) are necessary to produce homogeneous CNT solutions and layers.

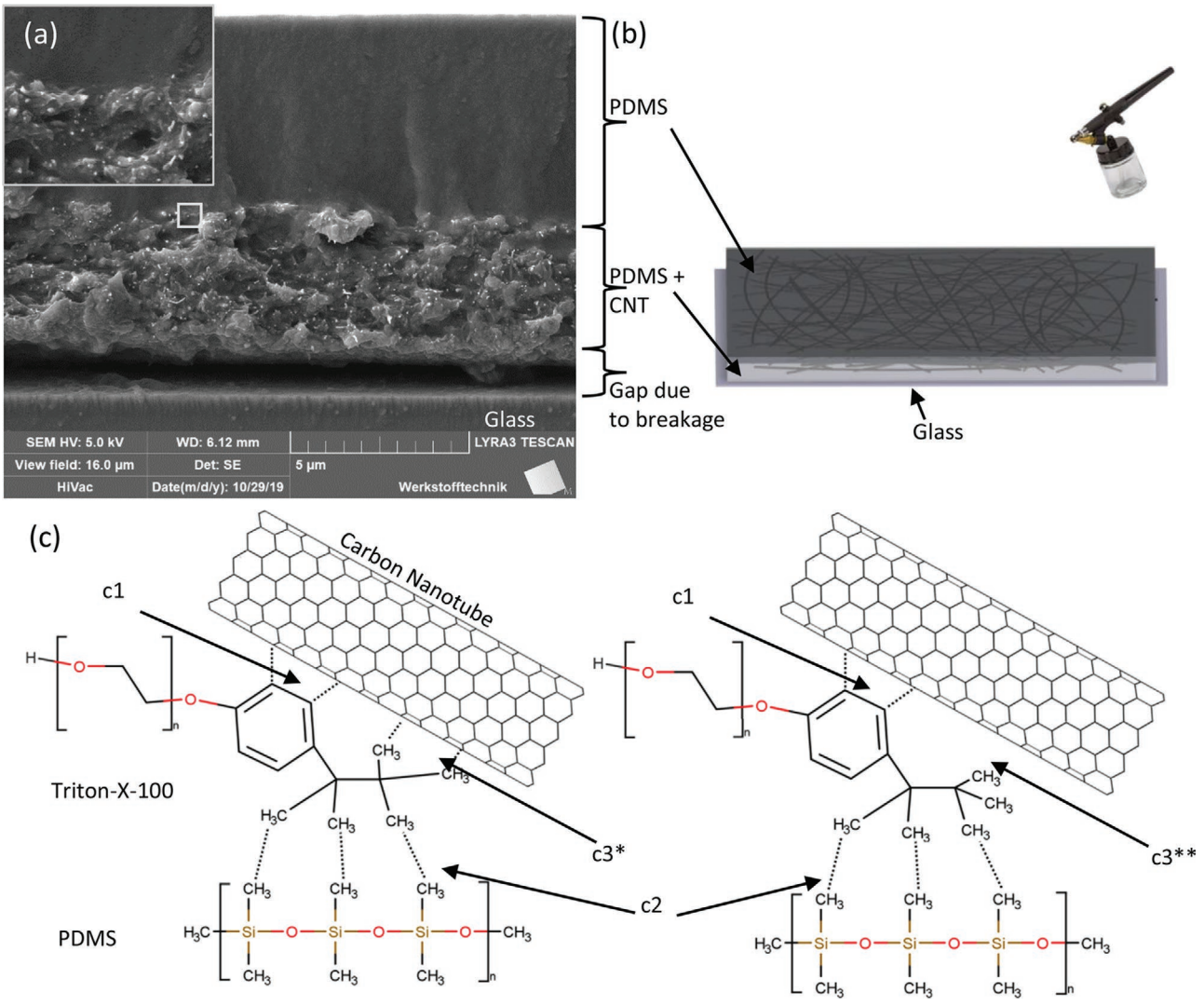

Figure 3. a) Final result of a spray coated MWCNT–PDMS composite after curing. b) Schematic drawing of a spray-coating process with an MWCNT–PDMS–Triton-X-100 solution on glass. c) Binding of Triton-X-100 with PDMS and MWCNT via pi-stacking c1), hydrogen bonds c2) and c3*/c3**) possible adsorption of the methyl groups on the surface of CNTs.

layers, the spraying time was between 5 and 20 min, which resulted in layer thicknesses between 0.9 and 32.2 µm. A PDMS curing agent solution based on a 0.1% Triton-X-100 water solution was applied to the layer using the same process to cure the composite. The ratio of PDMS to curing agent was 10:1. The layers created in this way were cured at over 100 °C for 30 min. The spraying process (Figure 3b) is robust, straightforward, and results in thin homogeneous layers in a short time (**Figures 3**a and **4**).

This study combines the binding capabilities of Triton-X-100 of both PDMS and MWCNT (Figure 3c). The methyl groups of the hydrophobic part of Triton-X-100 are able to connect to PDMS and MWCNTs. By adsorption, the methyl groups can attach to the MWCNTs, while hydrogen bonds are formed between the methyl groups of Triton-X-100 and the methyl groups of PDMS. The benzene ring can connect to the MWCNT via pi stacking. Bai et al.[58] and Geng et al.[57] described the adsorption and pi-stacking processes and the possible binding to the MWCNTs. This can result in adsorption of methyl groups on the surface of the MWCNT as well as in pi-stacking between the benzene rings of MWCNT and Triton-X-100.

The thicknesses of the spray-coated MWCNT–PDMS layers were measured with a Dektak 150 Surface Profiler. The reference point is on the coating free glass surface. The measured thicknesses were 0.9, 4.3, 10.2, and 32.2 µm, respectively.

The transmission coefficients of the layers were measured with an UV–vis spectrometer. Each sample shows low transmission (13.9–0.0%) at a wavelength of 1047 nm (**Figure 5**). As mentioned before (Figure 5a), PDMS shows a very high degree of transmission (91.2% at a wavelength of 630–1100 nm with a thickness of 1 mm, coated on glass).

3. Ultrasound Pressure Measurements

The ultrasound pressure in water was measured with a PVDF needle hydrophone (Imotec Messtechnik: type 80-0.5-4.0,

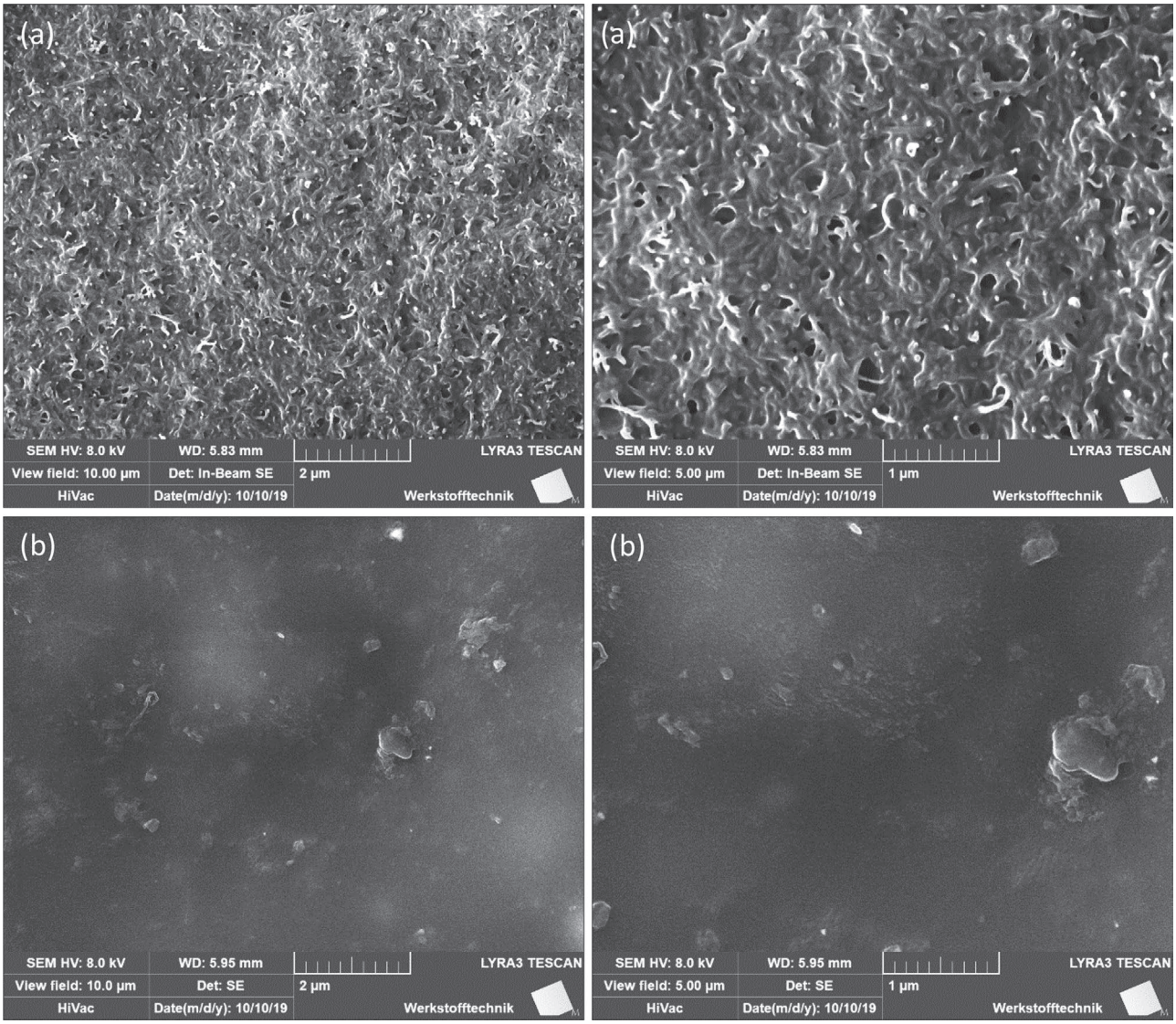

Figure 4. a) REM image of a CNT–PDMS layer in which the MWCNTs are very well enclosed by the PDMS polymer strands. A comparison with Figure 2 shows that all CNTs are processed without conglomerations. b) Inclusion of a CNT–PDMS layer, which is treated with a final protective layer. The impurities in (b) come from the manufacturing process, which was not carried out in a specific clean room.

1 mm diameter), which is calibrated up to 10 MHz. The measurement setup is shown in **Figures 6** and **7**a, and the received ultrasonic pulses are shown in **Figure 8**. A multimode fiber (1 mm diameter, 0.50 NA Step-Index Multimode Fiber FP1000URT from Thorlabs) was used for laser excitation, which was coupled with a fiber collimator (RC08FC-F01: Reflective Collimator, UV Enhanced, Ø 8.5 mm Beam, FC/PC). The used laser was a Q-switched laser (Mosquito Innolas, Krailling, Germany) with a wavelength of 1047 nm, a pulse duration of 11.4 ns, and a repetition rate of 1 kHz. The laser power was set at about 135 mW (fluency of 17.2 mJ cm^{-2}) for the 1 mm multimode fiber. A digital oscilloscope was used for data acquisition and signal processing. The distance between the layer excited by the laser and the hydrophone was 1 mm. The fiber end was directly adjusted on the rear side of the coated glass plate. In this work, the focus is the quick and robust manufacture of MWCNT–PDMS coatings. The hydrophone (bandwidth 10 MHz) can be well used for the characterization of the MWCNT–PDMS composites for ultrasonic applications in this frequency range.

The sound pressure measured in this way ranges from 1.7 to 3.4 MPa (see Figure 8a). The corresponding power spectra (Figure 8b), with maximum pressure referenced to 0 dB ranges from 6.6 to 9.7 MHz at a full width of quarter maximum (FWQM) bandwidth. The lower sound pressure at the 0.9 µm thin sample was caused by the fact that more transmission of the laser beam takes place, in this case a thin layer emits higher frequencies ultrasonic waves.[11,18,61] The relation of layer thicknesses with frequency ranges can be showed with the 32.2 µm thick sample, where the spectrum of 6.7 MHz differs significantly from the others ranging from 9.0 up to 9.7 MHz.[11,18,61] The sound pressure measured with

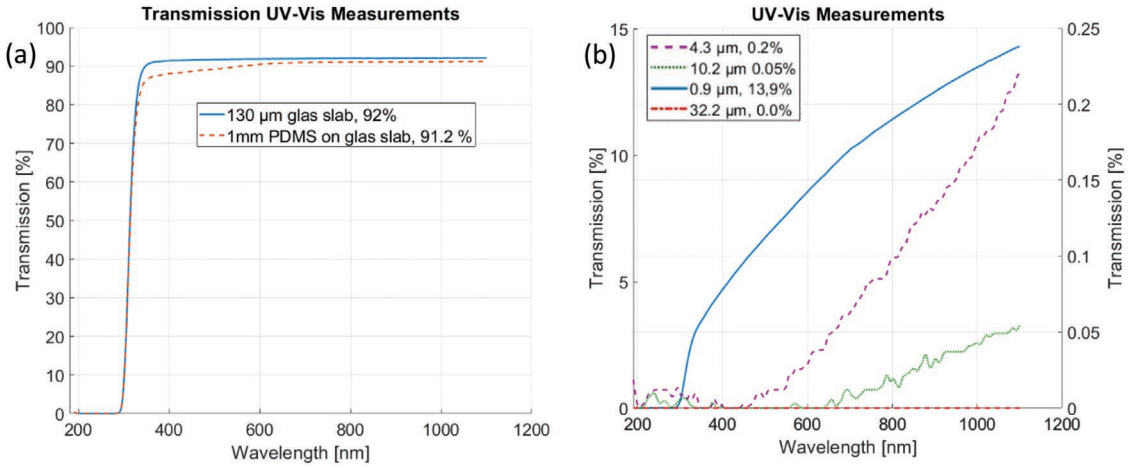

Figure 5. a) Transmission of the 130 µm thick glass slab (blue, solid line) and a 1 mm thick PDMS layer, which was coated on the glass slab (red, dotted line). b) The transmission curves of the thicker layers (green, red and purple (dotted lines)—right scale) show transmission values of less than 0.25% at a wavelength of 1047 nm. The 0.9 µm thick layer (blue, solid line—left scale) shows transmissions up to 13.9% at 1047 nm. All numerical values in the graphs are only valid for a wavelength of 1047 nm.

the 32.2 µm thick layer (Figure 8b) is not significantly higher (3.2 MPa), since the attenuation of the ultrasound pressure in thicker layers becomes stronger than within thinner layers.[18] Poduval et al. observed and describes similar effects, which explain the lower sound pressures at 0.9 and 32.2 µm.[41]

A further investigation is carried out to determine whether the MWCNT–PDMS layers meets the stability criteria in comparison with other methods. Baac et al. was able to determine a maximum fluency value of 477 mJ cm^{-2} of MWCNT–PDMS composite materials.[10] To significantly increase the fluency, a 200 µm multimode fiber (0.39 NA, Ø 200 µm core multimode optical fiber, high OH for 300–1200 nm, TECS Clad-FT200UMT from Thorlabs) was used (in our case a fluency of 400 mJ cm^{-2}). For ablation testing an MWCNT–PDMS layer was irradiated with the laser beam and optically investigated after each pass for ablation effects or other damages. The fluency was

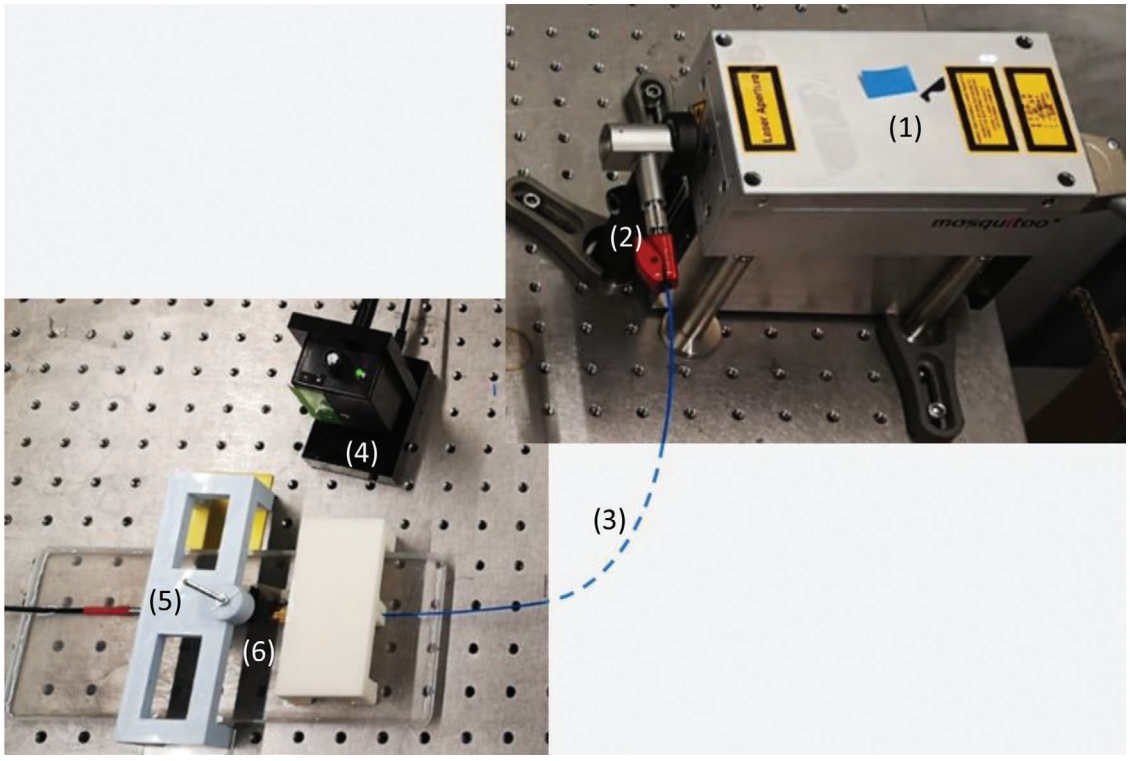

Figure 6. Measuring setup for determining the generated ultrasound pressure waves in water. The measuring distance from hydrophone to sample was ≈1 mm. Point (1) represents the optical source, which in (2) was coupled into a multimode fiber (3) and the laser pulses were conducted onto the sample (6). A photodiode (4) was used for triggering. The ultrasonic pressure waves were detected with the hydrophone (5).

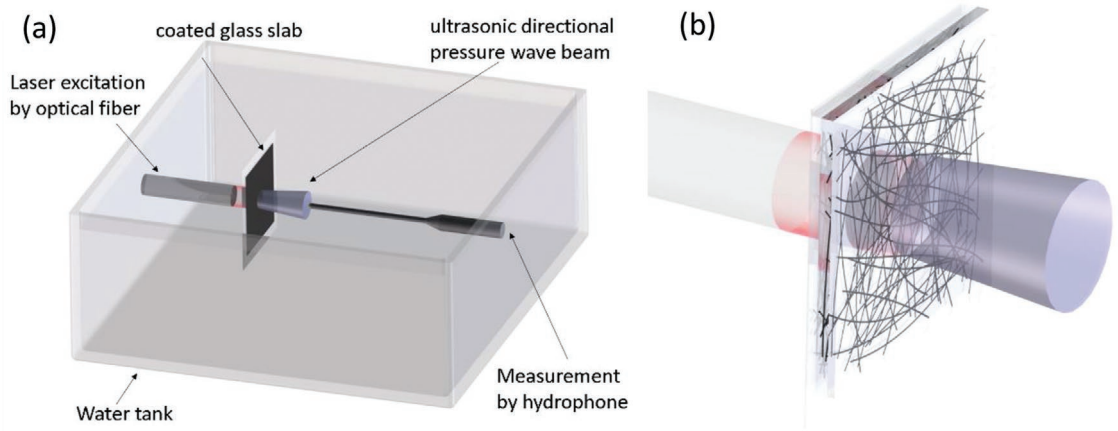

Figure 7. a) Measuring setup for the determination of the ultrasound pressure waves in water. The measuring distance was 1 mm and b) an enlarged schematic drawing of the CNT-based photoacoustic transmitter. The homogeneous MWCNTs heated by the laser pulses, transferred the heat immediately to the surrounding PDMS layer, which performs fast thermal expansions, and generated ultrasonic pressure waves in water.

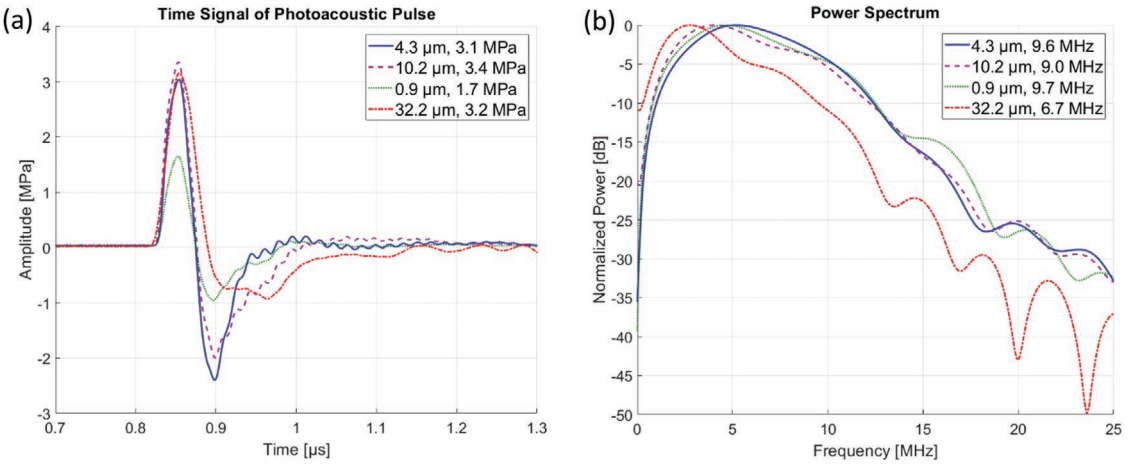

Figure 8. a) The generated ultrasound pressure ranges from 1.7 MPa for the 0.9 µm layer thickness to 3.4 MPa for the 10.2 µm layer thickness measured 1 mm from the end face of coated glass slab. b) The corresponding ultrasonic power spectra ranges from 6.6 to 9.7 MHz.

continuously increased until a visible damage occurs. The MWCNT–PDMS layers showed visible damage at a fluency of above 400 mJ cm^{-2}. The layers produced in this study correlate well with the damage thresholds in the literature. **Figure 9** shows the effect of damage caused by increased laser power.

In this work, a 1 mm fiber was used for the characterization of the functional layers. It is known that thinner fibers result in a higher fluency and the frequency bandwidth shifts toward a higher frequency range, as Hou et al.[62] described.

4. Conclusion

In conclusion, based on the study on the solubility of PDMS and the combination of MWCNT and PDMS in an aqueous Triton-X-100 solution, a MWCNT–PDMS composite can be successfully produced for ultrasonic wave generation. In the solution, the common binding capabilities of both MWCNT and PDMS were used via pi-stacking and adsorption of methyl groups directly to the MWCNT. The resulting solution can be

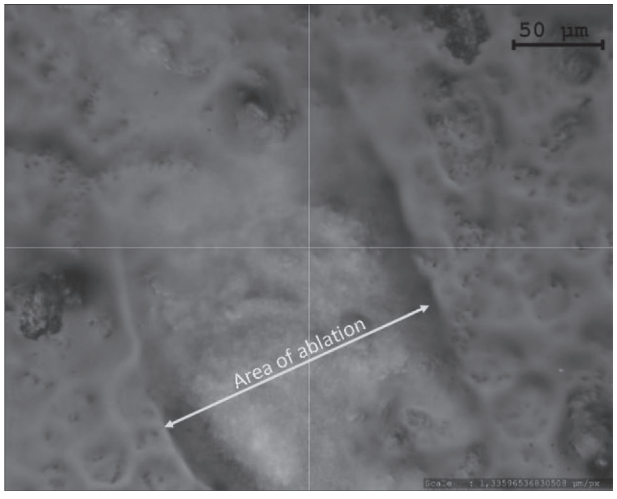

Figure 9. Image of the CNT–PDMS layer and the ablation that occurs at 400 mJ cm^{-2} with a 200 µm multimode fiber.

Table 1. Comparison and characterization of the previously manufactured multiwalled carbon nanotubes (MWCNT) with polydimethylsiloxane (PDMS) for photoacoustic transducers regarding to design, generated sound pressure, bandwidth and layer thickness, as well as the used laser.

Design, nanoparticle, polymer	Coating methodprocessing time [h]	Measuring distance [mm]	Layer thickness [µm] Bandwidth [MHz] Sound pressure [MPa]	Pulse duration [ns] Wavelength [µm] Fluency [mJ cm^{-2}]	Ref.
300 µm fiber, MWCNT, PDMS	Dip coating 24+	1.5	20 26.5 ≈4	2 1064 ≈36	Finlay et al.[a)]
200 µm fiber, MWCNT, PDMS	Dip coating 24+	3.1	20, 20 15, 20 4.5, 4	2, 2 1064, 1064 36.6, 96	Colchester et al.[b)]
200 µm fiber, MWCNT, PDMS	Dip coating 24+	2	20 ≈40 4.5	2 1064 36.1	Noimarket al.[c)]
Epoxy slab distal end of a 400 µm fiber, MWCNT, PDMS	Dip coating 24+	1.5	– 31.3 1.87	2 1064 8	Colchester et al.[b)]
Membrane, MWCNT, PDMS	Blade-coating 24+	9	46 27.2 ≈1	5 1064 76 µJ per pulse	Alles et al.[d)]
200 µm fiber, MWCNT, PDMS	Electrospinning, PDMS dip coating 48+	1.5	13.7 29 1.59	2 1064 35	Poduval et al.[e)]
Glas slab, MWCNT, PDMS	CVD, spin coating Few hours	1.4	2.6 80 –	3 532 43.4	Won Baac et al.[f)]
Coated PMMA film, MWCNT, PDMS	Vacuum filtration/transition, spin coating 16+	10	9 10 6.35	8 532 180 mW per pulse	Fan et al.[h)]
PET slab, MWCNT, PDMS	Vacuum filtration/transition, spin coating 16+	10	20 10 5.4	8 532 330 mJ per pulse	Fan et al.[h)]
PET lens, MWCNT, PDMS	Vacuum filtration/transition, spin coating 16+	14	20 10 35	8 532 330 mJ per pulse	Fan et al.[h)]
PMMA substrate, MWCNT, PDMS	Vacuum filtration method, Spin coating n.I.	10	5.2 15 3.2	8 532 180 mW cm^{-2}	Moon et al.[i)]
Coated lens, MWCNT, gold, PDMS	CVD, gold deposition, spin coating Few hours	5.5	2.6 30 57	6 532 42.4	Won Baac et al.[g)]
Coated lens, MWCNT, gold, PDMS	CVD, gold deposition, spin coating Few hours	9.2	16 25 70	6 532 9.6	Lee et al.[g)]

a) Ref. [50]; b) Refs. [2,51, 52]; c) Ref. [9]; d) Ref. [22]; e) Ref. [41]; f) Ref. [28]; g) Refs. [35,53]; h) Refs. [54,55]; i) Ref. [34].

sprayed precisely and convenient onto a thin glass plate with an airbrush gun, whereas the thicknesses of the layers can be easily controlled by the spraying time. Depending on their thicknesses (0.9–32.2 µm), the layers produced in this way show a low optical transmission rate of 13.9–0.0%. The ultrasonic measurements were performed with a hydrophone in a water tank. The ultrasound pressure levels (1.7–3.4 MPa) measured at 1 mm distance in water by using the current PVDF needle hydrophone are comparable with other photoacoustic actuators. For similar sound pressure levels (see **Table 1**), the fluency of the laser beam (17.2 mJ cm^{-2}) in our measurements is lower (36–96 mJ cm^{-2}) than the fluencies of other reported methods. The investigation results show the manufactured layers with this method are well suited for ultrasonic applications in medicine and in nondestructive material testing.

Supporting Information

Supporting Information is available from the Wiley Online Library or from the author.

Acknowledgements

The authors thank Prof. H. Huber for the use of the laser systems and Prof. C. Schindler for the permission to use the devices in her laboratory for microsystems technology, Dr. C. Eulenkamp for the support of the SEM pictures, and Mr. R. Laubinger for the support with the UV–vis spectrometer, and the research field "Micro-and Nano-Devices" of the Munich University of Applied Sciences.

Conflict of Interest

The authors declare no conflict of interest.

Keywords

laser-generated ultrasonic waves, multi-walled CNTs, nanocomposites, nanoparticles, photophysics, spray-coating methods

Received: December 13, 2019
Revised: January 31, 2020
Published online: March 3, 2020

[1] M. S. Mirza, Q. Liu, T. Yasin, X. Qi, J.-F. Li, M. Ikram, *Ceram. Int.* **2016**, *42*, 10745.
[2] R. J. Colchester, C. A. Mosse, D. S. Bhachu, J. C. Bear, C. J. Carmalt, I. P. Parkin, B. E. Treeby, I. Papakonstantinou, A. E. Desjardins, *Appl. Phys. Lett.* **2014**, *104*, 173502.
[3] C. Liu, F. T. Djuth, Q. Zhou, K. K. Shung, *IEEE Trans. Ultrason., Ferroelectr., Freq. Control* **2013**, *60*, 2615.
[4] J. S. Han, C. W. Gal, J. H. Kim, S. J. Park, *Ceram. Int.* **2016**, *42*, 9475.
[5] E. Biagi, F. Margheri, D. Menichelli, *IEEE Trans. Ultrason., Ferroelectr., Freq. Control* **2001**, *48*, 1669.
[6] T. Buma, M. Spisar, M. O'Donnell, *Appl. Phys. Lett.* **2001**, *79*, 548.
[7] N. Wu, Ye. Tian, X. Zou, V. Silva, A. Chery, X. Wang, *Opt. Soc. Am.* **2012**, *29*, 2016.
[8] W.-Y. Chang, W. Huang, J. Kim, S. Li, X. Jiang, *Appl. Phys. Lett.* **2015**, *107*, 161903.
[9] S. Noimark, R. J. Colchester, B. J. Blackburn, E. Z. Zhang, E. J. Alles, S. Ourselin, P. C. Beard, I. Papakonstantinou, I. P. Parkin, A. E. Desjardins, *Adv. Funct. Mater.* **2016**, *26*, 8390.
[10] H. W. Baac, J. G. Ok, T. Lee, L. J. Guo, *Nanoscale* **2015**, *7*, 14460.
[11] S. Noimark, R. J. Colchester, R. K. Poduval, E. Maneas, E. J. Alles, T. Zhao, E. Z. Zhang, M. Ashworth, E. Tsolaki, A. H. Chester, N. Latif, S. Bertazzo, A. L. David, S. Ourselin, P. C. Beard, I. P. Parkin, I. Papakonstantinou, A. E. Desjardins, *Adv. Funct. Mater.* **2018**, *28*, 1704919.
[12] Y. Tian, N. Wu, X. Zou, H. Felemban, C. Cao, X. Wang, *Opt. Eng.* **2013**, *52*, 065005.
[13] H. W. Baac, T. Ling, S. Ashkenazi, S.-W. Huang, L. J. Guo, *Proc. SPIE* **2010**, *7564*, 75642M.
[14] M.-A. Park, S. H. Lee, J. J. Yoh, *Appl. Phys. B* **2013**, *113*, 389.
[15] T. Lee, L. J. Guo, *Adv. Opt. Mater.* **2017**, *5*, 1600421.
[16] V. V. Kozhushko, P. Hess, *Appl. Phys. Lett.* **2007**, *91*, 224107.
[17] Y. Hou, J.-S. Kim, S. Ashkenazi, S.-W. Huang, L. J. Guo, M. O'Donnell, *Appl. Phys. Lett.* **2007**, *91*, 073507.
[18] T. Buma, M. Spisar, M. O'Donnell, *IEEE Trans. Ultrason., Ferroelectr., Freq. Control* **2003**, *50*, 1161.
[19] S.-Y. Hung, W.-S. Wu, B.-Y. Hsieh, P.-C. Li, *J. Biomed. Opt.* **2015**, *20*, 1.
[20] N. Wu, Y. Tian, X. Zou, X. Wang, *SPIE Proc.* **2013**, *8694*, 1.
[21] X. Zou, N. Wu, Y. Tian, X. Wang, *Opt. Express* **2014**, *22*, 18119.
[22] E. J. Alles, S. Noimark, E. Maneas, E. Z. Zhang, I. P. Parkin, P. C. Beard, A. E. Desjardins, *Biomed. Opt. Express* **2018**, *9*, 3481.
[23] B.-Y. Hsieh, J. Kim, J. Zhu, S. Li, X. Zhang, X. Jiang, *Appl. Phys. Lett.* **2015**, *106*, 021902.
[24] Y. Hou, S. Ashkenazi, S.-W. Huang, M. O'Donnell, *IEEE Trans. Ultrason., Ferroelectr., Freq. Control* **2007**, *54*, 682.
[25] Y. Li, Z. Guo, G. Li, S.-L. Chen, *Opt. Express* **2018**, *26*, 21700.
[26] W.-Y. Chang, X. A. Zhang, J. Kim, W. Huang, A. Bagal, C.-H. Chang, T. Fang, H. F. Wu, X. Jiang, *IEEE Trans. Nanotechnol.* **2018**, *17*, 985.
[27] J. Kim, H. Kim, W.-Y. Chang, W. Huang, X. Jiang, P. A. Dayton, *IEEE Nanotechnol. Mag.* **2019**, *13*, 13.
[28] H. Won Baac, J. G. Ok, H. J. Park, T. Ling, S.-L. Chen, A. J. Hart, L. J. Guo, *Appl. Phys. Lett.* **2010**, *97*, 234104.
[29] K Mizunoa, J Ishiib, H Kishidac, Y Hayamizua, S Yasudaa, D N. Futabaa, M Yumuraa, K Hataa, *Proc. Natl. Acad. Sci. USA* **2009**, *106*, 6044.
[30] X. J. Wang, J. D. Flicker, B. J. Lee, W. J. Ready, Z. M. Zhang, *Nanotechnology* **2009**, *20*, 215704.
[31] T. de Los Arcos, P. Oelhafen, D. Mathys, *Nanotechnology* **2007**, *18*, 265706.
[32] K. Cui, B. L. Wardle, *ACS Appl. Mater. Interfaces* **2019**, *11*, 35212.
[33] N. Bowden, W. T. S. Huck, K. E. Paul, G. M. Whitesides, *Appl. Phys. Lett.* **1999**, *75*, 2557.
[34] C. Moon, X. Fan, K. Ha, D. Kim, *AIP Adv.* **2017**, *7*, 015107.
[35] H. W. Baac, J. G. Ok, A. Maxwell, K.-T. Lee, Y.-C. Chen, A. J. Hart, Z. Xu, E. Yoon, L. J. Guo, *Sci. Rep.* **2012**, *2*, 989.
[36] D. K. Cai, A. Neyer, R. Kuckuk, H. M. Heise, *Opt. Mater.* **2008**, *30*, 1157.
[37] N. E. Stankova, P. A. Atanasov, R.G. Nikov, R. G. Nikov, N. N. Nedyalkov, T. R. Stoyanchov, N. Fukata, K. N. Kolev, E. I. Valova, J. S. Georgieva, S.A. Armyanov, *Appl. Surf. Sci.* **2016**, *374*, 96.
[38] J. Hong, J. Lee, C. K. Hong, S. E. Shim, *Curr. Appl. Phys.* **2010**, *10*, 359.
[39] C.-X. Liu, J.-W. Choi, *Nanomaterials* **2012**, *2*, 329.
[40] M. Sianipar, S. H. Kim, K. Khoiruddin, F. Iskandar, I. G. Wenten, *RSC Adv.* **2017**, *7*, 51175.
[41] R. K. Poduval, S. Noimark, R. J. Colchester, T. J. Macdonald, I. P. Parkin, A. E. Desjardins, I. Papakonstantinou, *Appl. Phys. Lett.* **2017**, *110*, 223701.
[42] G. Ciofani, V. Raffa, V. Pensabene, A. Menciassi, P. Dario, *Fullerenes, Nanotubes, Carbon Nanostruct.* **2009**, *17*, 11.
[43] Y. Y. Huang, E. M. Terentjev, *Polymers* **2012**, *4*, 275.
[44] J. N. Coleman, U. Khan, W. J. Blau, Y. K. Gun'ko, *Carbon* **2006**, *44*, 1624.
[45] F. Fei Fang, H. Jin Choi, J. Joo, *J. Nanosci. Nanotechnol.* **2008**, *8*, 1559.
[46] S. S. Ray, S. Vaudreuil, A. Maazouz, M. Bousmina, *J. Nanosci. Nanotechnol.* **2006**, *6*, 2191.
[47] Y. Y. Huang, T. P. J. Knowles, E. M. Terentjev, *Adv. Mater.* **2009**, *21*, 3945.
[48] A. Lucas, C. Zakri, M. Maugey, M. Pasquali, P. van der Schoot, P. Poulin, *J. Phys. Chem. C* **2009**, *113*, 20599.
[49] S. Guan, S. Song, H. Li, G. Mo, S. Zhao, L. Guo, *Mater. Lett.* **2018**, *216*, 281.
[50] M. C. Finlay, C. A. Mosse, R. J. Colchester, S. Noimark, E. Z. Zhang, S. Ourselin, P. C. Beard, R. J. Schilling, I. P. Parkin, I. Papakonstantinou, A. E. Desjardins, *Light: Sci. Appl.* **2017**, *6*, e17103.
[51] R. J. Colchester, C. A. Mosse, D. I. Nikitichev, E. Z. Zhang, S. West, P. C. Beard, I. Papakonstantinou, A. E. Desjardins, *SPIE Proc.* **2015**, *9323*, 1.
[52] R. J. Colchester, C. Little, G. Dwyer, S. Noimark, E. J. Alles, E. Z. Zhang, C. D. Loder, I. P. Parkin, I. Papakonstantinou,

P. C. Beard, M. C. Finlay, R. D. Rakhit, A. E. Desjardins, *Sci. Rep.* **2019**, *9*, 5576.
[53] T. Lee, J. G. Ok, L. J. Guo, H. W. Baac, *Appl. Phys. Lett.* **2016**, *108*, 104102.
[54] X. Fan, Y. Baek, K. Ha, M. Kim, J. Kim, D. Kim, H. W. Kang, J. Oh, *Jpn. J. Appl. Phys.* **2017**, *56*, 07JB05.
[55] X. Fan, K. Ha, M. Kim, G. Kang, M. J. Choi, J. Oh, *Jpn. J. Appl. Phys.* **2018**, *57*, 07LB10.
[56] H. Wang, W. Zhou, D. L. Ho, K. I. Winey, J. E. Fischer, C. J. Glinka, E. K. Hobbie, *Nano Lett.* **2004**, *4*, 1789.
[57] Y. Geng, M. Y. Liu, J. Li, X. M. Shi, J. K. Kim, *Composites, Part A* **2008**, *39*, 1876.
[58] Y. Bai, D. Lin, F. Wu, Z. Wang, B. Xing, *Chemosphere* **2010**, *79*, 362.
[59] R. Rastogi, R. Kaushal, S. K. Tripathi, A. L. Sharma, I. Kaur, L. M. Bharadwaj, *J. Colloid Interface Sci.* **2008**, *328*, 421.
[60] L. Vaisman, G. Marom, H. D. Wagner, *Adv. Funct. Mater.* **2006**, *16*, 357.
[61] E. J. Alles, J. Heo, S. Noimark, R. J. Colchester, I. P. Parkin, H. W. Baac, A. E. Desjardins, *IEEE Int. Ultrason. Symp.* **2017**, 1.
[62] Y. Hou, S. Ashkenazi, S.-W. Huang, M. O'Donnell, *IEEE Trans. Ultrason., Ferroelectr., Freq. Control* **2008**, *55*, 2719.